Int. J. Electrochem. Sci., 5 **(2010)** 867 - 879

International Journal of
ELECTROCHEMICAL
SCIENCE
www.electrochemsci.org

Experimental and Computational Study on Electrochemical Oxidation of Catechols

Davood Nematollahi[1,*] *, Avat (Arman) Taherpour*[2]*, Saeed Jameh-Bozorghi*[2]*, Ailine Mansouri*[2]*, Bita Dadpou*[2]

[1] Faculty of Chemistry, Bu-Ali Sina University, Zip Code: 65178-38683, Hamedan, Iran.
Tel.: +98 811 8282807, fax: +98 811 8257407. E-mail: nemat@basu.ac.ir.
[2] Chemistry Department, Faculty of Science, Islamic Azad University, Arak Branch, P.O.Box 38135-567, Arak, Irane
[*]E-Mail: nemat@basu.ac.ir

Received: 26 May 2010 / *Accepted:* 12 June 2010 / *Published:* 20 June 2010

In this work, catechol and some of its derivatives have been studied by means of cyclic voltammetry on a glassy carbon electrode in aqueous solution containing phosphate buffer (pH 2.0) as supporting electrolyte. The measurements were done at room temperature. The chemical structure of 16 catechol derivatives has been optimized by using of Gaussian 98 program and Quantum Mechanical Calculation Ab Initio. Optimization was performed at the #B3LYP/6-311+G** level. The half-wave potentials ($E_{1/2}$), were correlated with the calculated energies of the highest occupied molecular orbital (E_{HOMO}) and the lowest unoccupied molecular orbital (E_{LUMO}) of the compounds studies. The linear relationship between $E_{1/2}$ and E_{HOMO} (or $E_{1/2}$ and E_{LUMO}), of a series of compounds, demonstrates that they have a similar mechanism of the electron transfer reaction.

Keywords: catechol, cyclic voltammetry, gaussian 98, HOMO, DFT theory, B3LYP.

1. INTRODUCTION

Among many electrochemical techniques presented for the study of chemical reactions, cyclic voltammetry has become a very popular technique for initial electrochemical studies of new systems. It is easy to apply experimentally, readily available in commercial instruments and has proven as very useful tool in obtaining information about fairly complicated electrode reactions. In addition, among the organic compounds, catechols can be easily oxidized to the corresponding reactive *o*-benzoquinones mainly due to their low oxidation potentials. It is worth mentioning that catechols are used in a variety of applications including photography, dying, rubber and plastic production and

pharmaceutical industry [1]. In addition, catechol derivatives play an important role in mammalian metabolism, and many compounds of this type are known to be secondary metabolites of higher plants. In addition, many drugs such as doxorubicin, daunorubicin and mitomycin C that are used in cancer chemotherapy contain quinones [2]. Furthermore, catechol derivatives are a promising group of compounds which may lead to the discovery of selective acting, biodegradable agrochemicals having high human, animal and plant compatibility and, thus, worthwhile for further investigation [3].

So, in this work, the chemical structure of some catechol derivatives (Fig. 1) has been optimized by using of Gaussian 98 program and Quantum Mechanical Calculation Ab Initio. Optimization was performed at the #B3LYP/6-311+G** level and the half-wave potentials obtained from cyclic voltammograms, were correlated with the calculated energies of the highest occupied molecular orbital (E_{HOMO}) and the lowest unoccupied molecular orbital (E_{LUMO}) of the compounds studies.

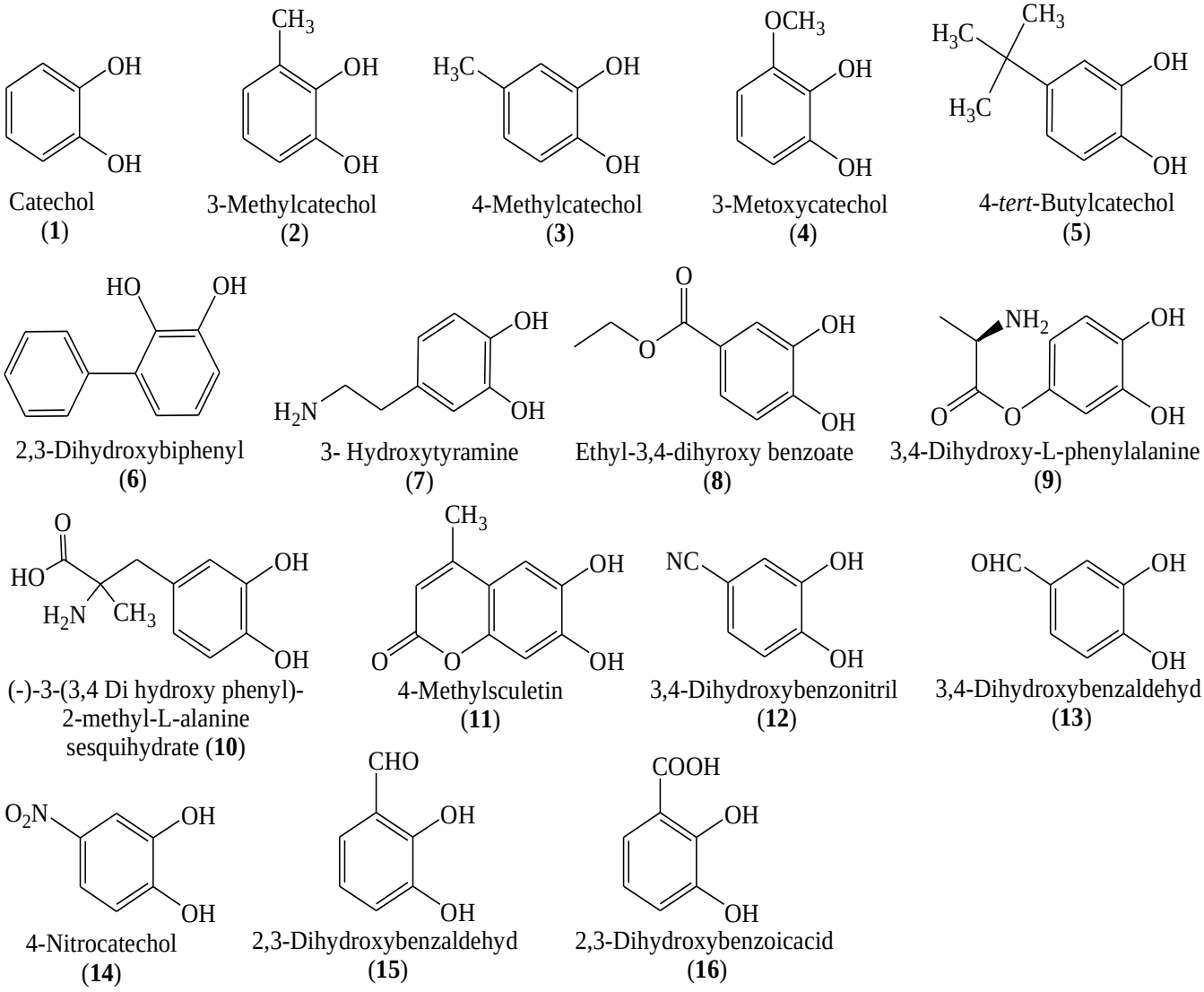

Figure 1. Chemical structure of the studied catechols **1-16**.

2. EXPERIMENTAL PART

2.1. Apparatus and reagents

Cyclic voltammetry was performed using Sama500 potentiostat/galvanostat. The working electrode used in the voltammetry experiments was a glassy carbon disc (1.8 mm diameter) and platinum wire was used as the counter electrode. The working electrode potentials were measured versus standard calomel electrode (SCE) (all electrodes from AZAR Electrode). All chemicals (catechols and phosphate salts) were reagent-grade materials, from Aldrich and E. Merck, respectively. These chemicals were used without further purification. The half-wave potentials ($E_{1/2}$) were calculated as the average of the anodic and cathodic peak potentials of the cyclic voltammograms ((E_{pa}+E_{pc})/2. All experiments were carried out at room temperature.

2.2. Computational details

DFT (density functional theory) calculations were carried out using #B3LYP/6-311+G** level of theory with the GAUSSIAN 98 package of programs implemented on a Pentium-PC computer with a 2.6 GHz processor. Initial estimation of the structural geometry of the compounds **1-16** was obtained by a molecular mechanic program PCMODEL (88.0) and for further optimization of geometry, we used the PM3 method of the MOPAC 7.0 computer program. The GAUSSIAN 98 package of programs were finally used to perform DFT calculations at the #B3LYP/6-311+G** level. Energy-minimum molecular geometries were located by minimizing energy, with respect to all geometrical coordinates without imposing any symmetrical constraints. The nature of the stationary points for the compounds **1-16** has been fixed by means of the number of imaginary frequencies. For minimum state structure, only real frequency values, and in the transition-state, only single imaginary frequency values were accepted. NBO analysis was then performed at the #B3LYP/6-311+G** level by the NBO 3.1 program included in the GAUSSIAN 98 package of programs.

3. RESULTS AND DISCUSSION

3.1. Voltammetric studies

Figure 2, shows the voltammetric curves obtained for the oxidation of catechol (**1**) (1 mM) in water containing phosphate buffer (c = 0.2 M, pH = 2.0) at various scan rates, at a glassy carbon electrode. In the studied potential range, a well-defined voltammetric curve is obtained that has an anodic (A_1) and the corresponding cathodic (C_1) peaks. These peaks correspond to the oxidation of catechol (**1**) to *o*-benzoquinone (**1a**) and vice versa within a quasi-reversible two-electron process (Scheme 1) [4-6]. Under these conditions, peak current ratio (I_p^{C1}/I_p^{A1}) is nearly unity, particularly during the repetitive cycling of potential, can be considered as a criterion for the stability of *o*-benzoquinone produced at the surface of the electrode under the experimental conditions. In other

words, any hydroxylation, dimerization or oxidative ring cleavage reactions are too slow to be observed on the time scale of cyclic voltammetry [7-13].

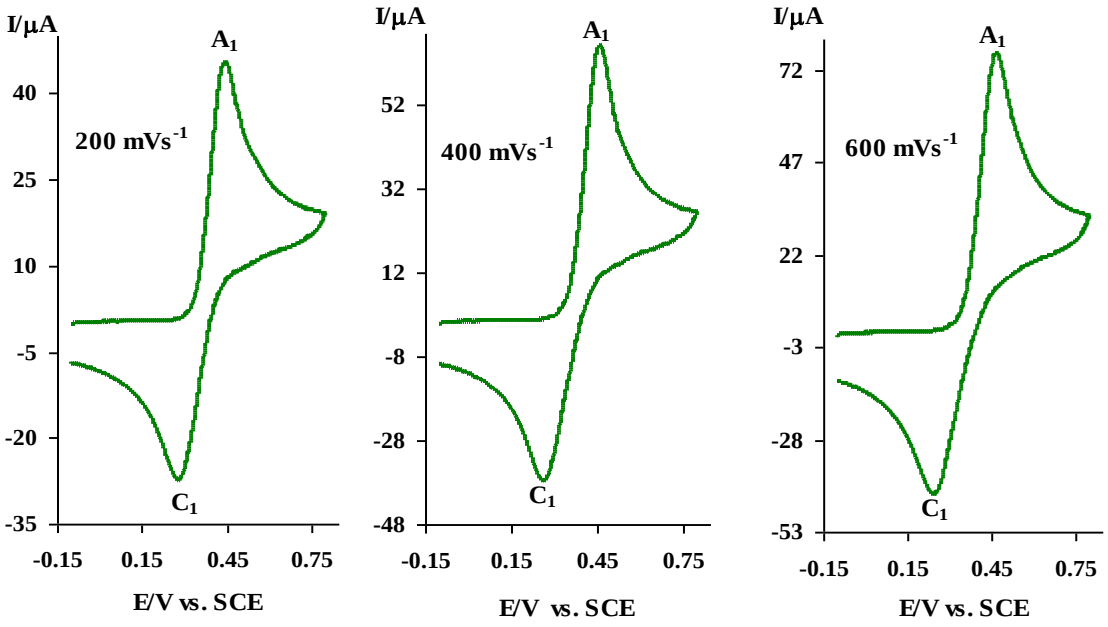

Figure 2. Typical cyclic voltammograms of 1 mM catechol (**1**) at a glassy carbon electrode, in aqueous solution containing 0.2 M phosphate buffer (pH 2.0). Scan rates are 200, 400, and 600 mV s^{-1}, respectively. t = 25±1 ˚C.

The same results obtained for electrochemical oxidation of other catechols such as: 3-methylcatechol (**2**), 4-methylcatechol (**3**), 3-methoxycatechol (**4**), 4-*tert*-butylcatechol (**5**), 2,3-dihydroxybiphenyl (**6**), 3-hydroxytyramine (**7**), 3,4-dihydroxy-L-phenylalanine (**8**), 3-(3,4-dihydroxyphenyl)-2-methyl-L-alanine (**9**) and 4-methylsculetin (**10**). Figure 3, shows the cyclic voltammograms of catechols **2-10** (1 mM) in water containing phosphate buffer (*c* = 0.2 M, pH = 2.0). As can be seen, a well-defined voltammetric curve with an anodic (A_1) and the corresponding cathodic (C_1) is obtained in each case. These peaks correspond to the oxidation of catechol **2-10** to *o*-benzoquinone **2a-10a** and vice versa [4-6].

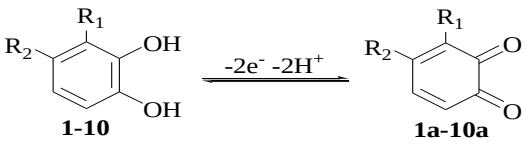

$R_1 = R_2 = H$ (1)
$R_1 = H$, $R_2 = CH_3$ (**3**)
$R_1 = H$, R_2 = *tert*-Butyl (**5**)
$R_1 = H$, $R_2 = CH_2\text{-}CH_2\text{-}NH_2$ (**7**)

$R_1 = CH_3$, $R_2 = H$ (**2**)
$R_1 = OCH_3$, $R_2 = H$ (**4**)
R_1 = Phenyl, $R_2 = H$ (**6**)

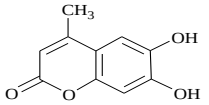

(**10**)

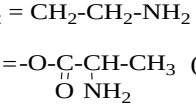

($R_1 = H$, $R_2 =$ -O-C(=O)-CH(NH$_2$)-CH$_3$ (**8**))

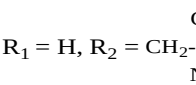

($R_1 = H$, $R_2 = CH_2$-C(CH$_3$)(NH$_2$)-COOH (**9**))

Scheme 1.

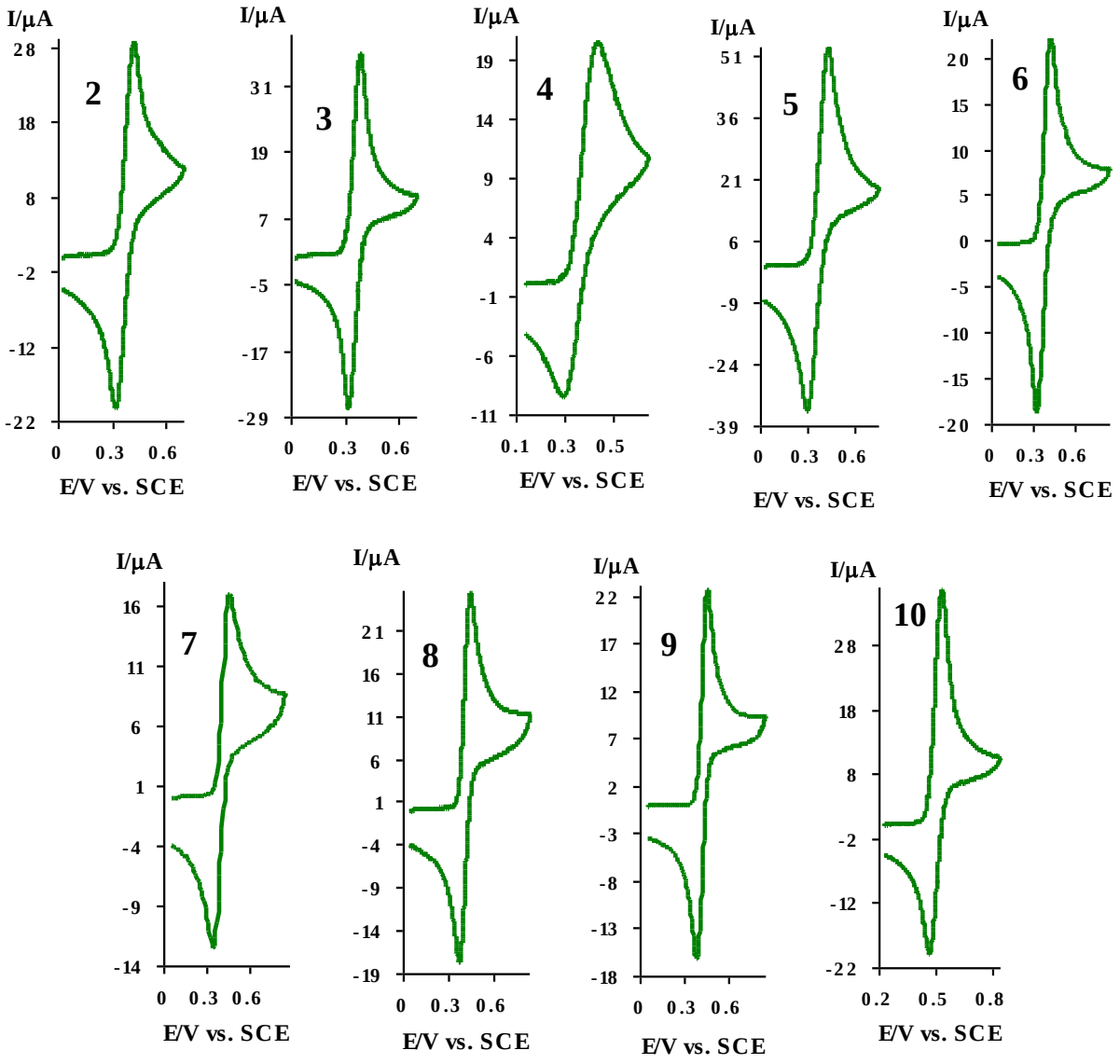

Figure 3. Cyclic voltammograms of 1 mM; 3-methylcatechol (**2**), 4-methylcatechol (**3**), 3-methoxycatechol (**4**), 4-*tert*-butylcatechol (**5**), 2,3-dihydroxybiphenyl (**6**), 3-hydroxytyramine (**7**), 3,4-dihydroxy-*L*-phenylalanine (**8**), 3-(3,4-dihydroxyphenyl)-2-methyl-*L*-alanine (**9**), 4-methylsculetin (**10**) at a glassy carbon electrode, in aqueous solution containing 0.2 M phosphate buffer (pH 2.0). Scan rate; 200 mV s^{-1}. t = 25±1 ˚C.

Another type of catechols is catechols with electron-withdrawing groups (Figure 4). These catechols consist of ethyl-3,4-dihydroxybenzoate (**11**), 3,4-dihydroxybenzonitril (**12**), 3,4-dihydroxybenzaldehyd (**13**), 2,3-dihydroxybenzaldehyd (**14**), 4-nitrocatechol (**15**) and 2,3-dihydroxybenzoic acid (**16**). In this type of catechols, the peak current ratio (I_p^{C1}/I_p^{A1}) is less than unity and decreases with increasing pH as well as by decreasing the potential sweep rate. These can be related to the coupling of anionic or dianionic forms of catechols with *o*-benzoquinones (dimerization reaction) [7,8], hydroxylation [9-11] and/or oxidative ring cleavage (Scheme 2) [12,13].

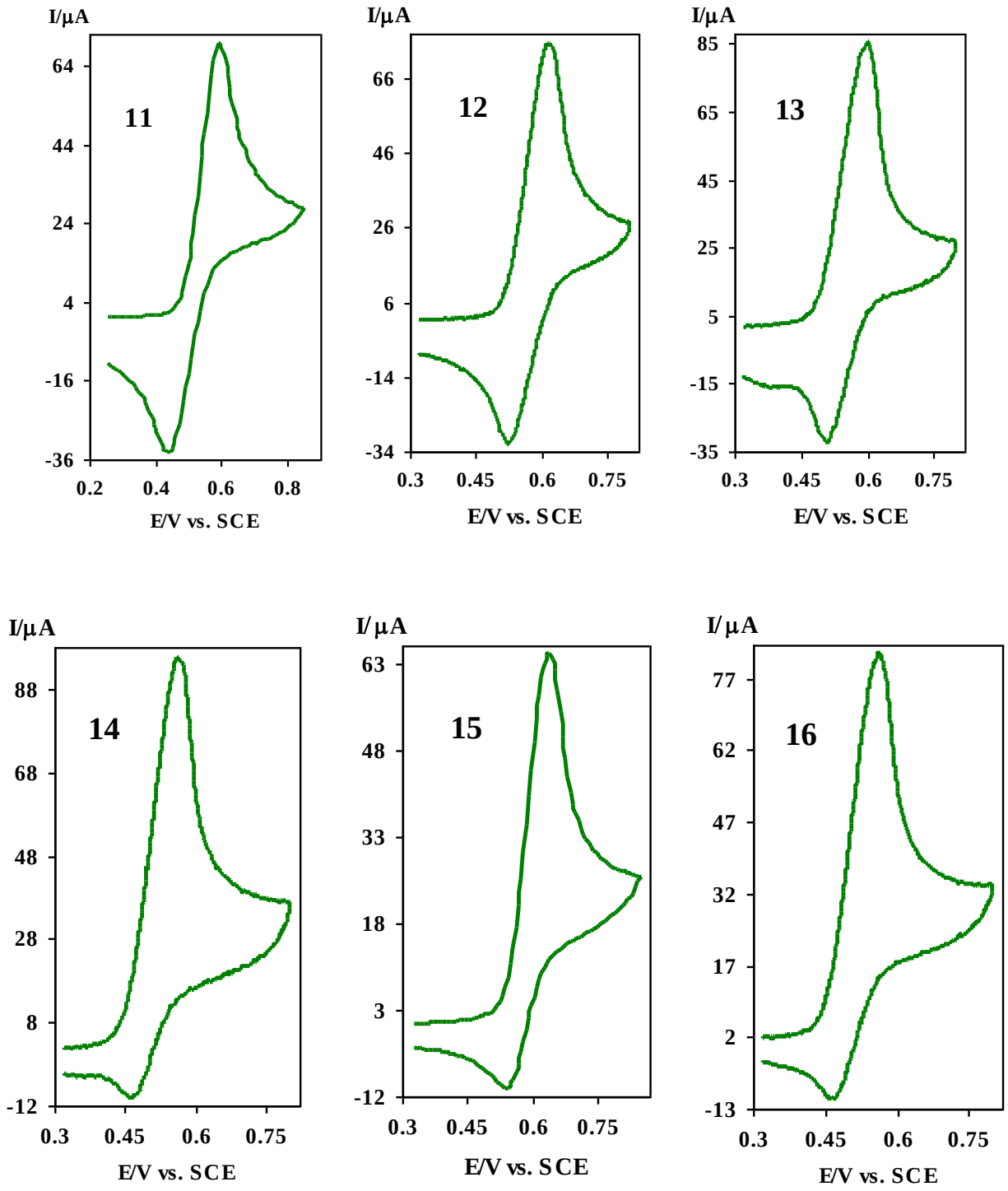

Figure 4. Cyclic voltammograms of 1 mM; ethyl-3,4-dihydroxybenzoate (**11**), 3,4-dihydroxybenzonitril (**12**), 3,4-dihydroxybenzaldehyd (**13**), 2,3-dihydroxybenzaldehyd (**14**), 4-nitrocatechol (**15**) and 2,3-dihydroxybenzoic acid (**16**) at a glassy carbon electrode, in aqueous solution containing 0.2 M phosphate buffer (pH 2.0). Scan rate; 600 mV s^{-1}. t = 25±1 ˚C.

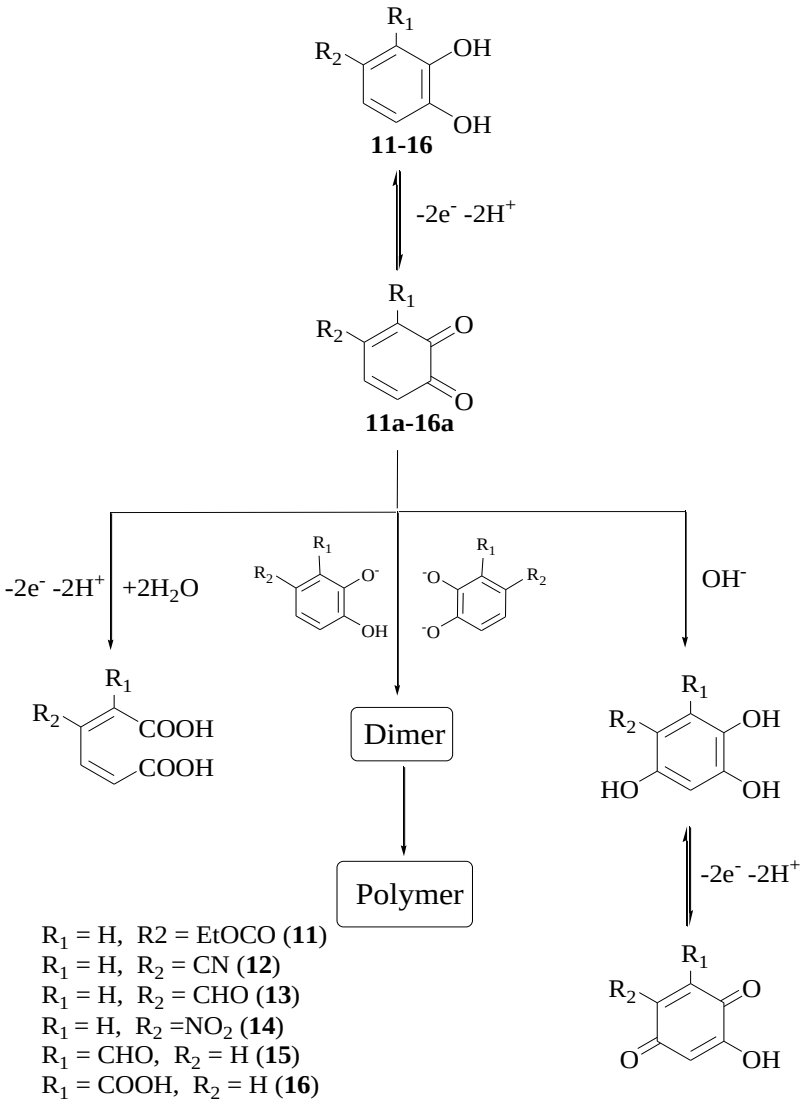

Scheme 2.

3.2. Computational studies

Here, we wish to present the calculated energies of the HOMO and LUMO of catechol derivatives as shown in Fig. 1. As has been shown earlier, for benzendiol derivatives the prevailing mechanism consists of a formation of a radical cation, as the primary reaction stage [14,15]:

$$QH_2 - e \rightleftharpoons [QH_2]^{\cdot +}$$

where QH_2 is the substrate, and $[QH_2]^{\cdot +}$ is the radical cation, which has an unpaired spin and a positive charge at the same time. When QH_2 is oxidized to form radical cation, $[QH_2]^{\cdot +}$, it donates an electron from its highest occupied molecular orbital (HOMO). On the other hand, when $[QH_2]^{\cdot +}$ is reduced to QH_2, it accepts an electron into its lowest unoccupied molecular orbital (LUMO).

Alternatively, in reductions of quinones, the first step is usually a one-electron process that produces a radical anion, $Q^{\cdot -}$[15,16]:

$$Q + e \rightleftharpoons Q^{\cdot -}$$

Following Sasaki et al. [17] and Saeva and Olin [18], the correlation between the calculated energies of the HOMO and LUMO and the electrode potentials of the catechols shown in Fig. 1 (compounds **1-16**) have been investigated. The chemical structure of catechols **1-16** has been optimized by using of Gaussian 98 program and Quantum Mechanical Calculation Ab Initio. Optimization was performed at the #B3LYP/6-311+G** level. Simple relations have been found between the potential of anodic peak (E_{pa}) and energy of the HOMO (E_{HOMO}) and half-wave potential ($E_{1/2}$) and E_{HOMO} (or E_{LUMO}). These relations are also shown in Figs. 5 and 6. The relation between half-wave potential, ($E_{1/2}$) and energy of the lowest unoccupied level of the catechols is also justified since the molecules **1-16** accepts an electron to be converted to the reduced form [16,18]. Also, the linear relationship between $E_{1/2}$ and E_{HOMO} (or E_{LUMO}) for a series of compounds, demonstrates that they have a similar mechanism of the electron transfer reaction. If there is no correlation between the measured potentials (E_{pa}, or $E_{1/2}$) and the calculated E_{HOMO} or E_{LUMO}, then, it may mean that there is a change of the mechanism of the electron transfer reaction [19-24].

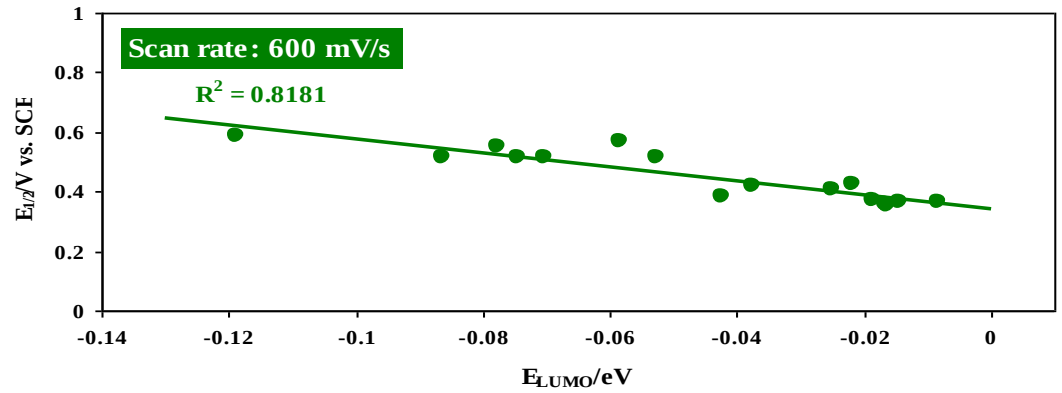

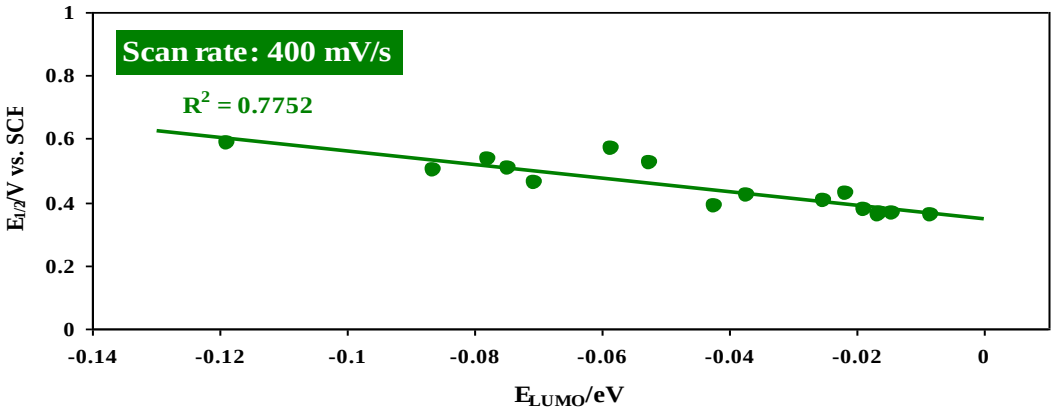

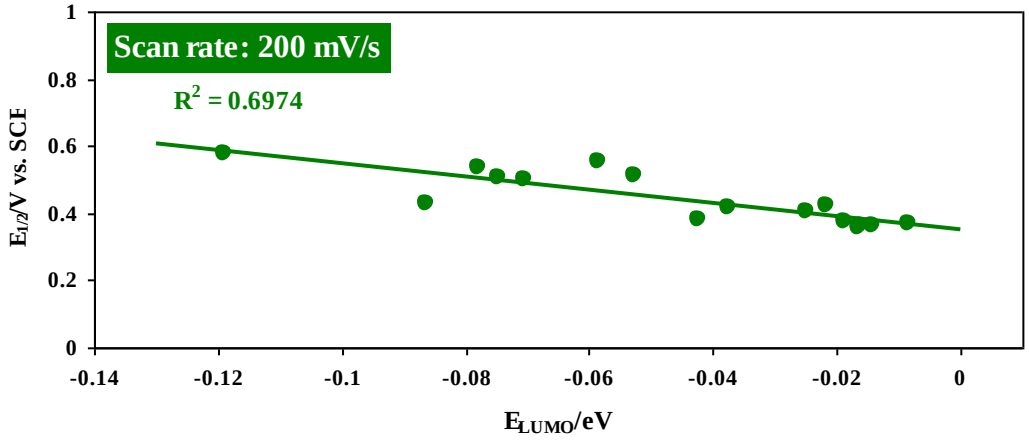

Figure 5. Half-wave potentials ($E_{1/2}$) of catechols *vs.* LUMO energies at scan rates; 600, 400 and 200 mV/s.

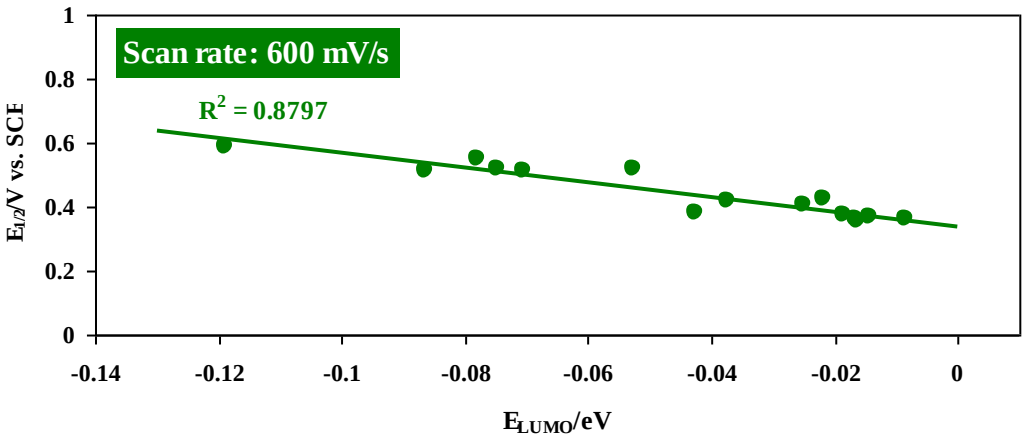

Figure 6. Half-wave potentials ($E_{1/2}$) of catechols *vs.* LUMO energies at scan rate 600 mV/s, calculated without 3,4-dihydroxybenzonitril (**12**).

Table 1. The relations between $E_{1/2}$ of catechols **1-16** and E_{LUMO} in various scan rates.

Equation	Scan rate (mV/s)	Equation	R^2
1	200	$E_{1/2} = 0.3487 - 1.9945E_{LUMO}$	0.6974
2	400	$E_{1/2} = 0.3445 - 2.1696E_{LUMO}$	0.7752
3	600	$E_{1/2} = 0.3417 - 2.3646E_{LUMO}$	0.8181
4[a]	600	$E_{1/2} = 0.3392 - 2.2911E_{LUMO}$	0.8797[a]

[a]Without 3,4-dihydroxybenzonitril (**12**).

As Table 1 shows, the regression coefficient (R^2) increases with increasing scan rate. R^2 is indicating goodness-of-fit of the regression. This is expected because of the change of $E_{1/2}$ at different scan rates when electrode reaction is in accompany with coupled homogeneous chemical reactions [25]. As Scheme 2 shows, electrochemically generated *o*-benzoquinones **1a-16a**, participate in following chemical reactions [4-6]. An important parameter in determining the effect of chemical reaction is the ratio of rate constant of chemical reaction to the potential scan rate, k/v, where k is rate constant of chemical reaction of electrochemically generated *o*-benzoquinones **1a-16a** and v is potential scan rate. Our previous works indicates that the generated *o*-benzoquinones from catechols with electron-withdrawing groups have great tendency for participation in following chemical reactions [26-30]. In kinetic and partially intermediate conditions (when k is large and/or v is low) $E_{1/2}$ shifts toward negative potentials [25], and the extent of this shift for various catechols is related to rate constant of chemical reaction, k. The deviation of $E_{1/2}$ from its reversible (actual) amount in lower scan rates caused the decreasing of R^2. In the case of 3,4-dihydroxybenzonitril (**12**), because of the higher reactivity of its *o*-benzoquinone **12a** produces a larger error. Therefore, in Table 1, Eq. 4, removing of 3,4-dihydroxybenzonitril (**12**), caused an increase in the R^2.

Table 2, shows the relations between $E_{1/2}$ (or E_{pa}) and E_{HOMO} in v = 600 mV/s. The relation between half-wave potential ($E_{1/2}$) or anodic electrode potential (E_{pa}) with energy of the highest occupied molecular level of the molecule (HOMO) is reasonable since the molecule **1-16** has already gained an electron. Comparison of regression coefficient (R^2) of Eq. 5 (0.5589) with Eq. 6 (0.8394) (or Eq. 7 with Eq. 8) in Table 2, shows that removing of 4-methylcatechol (**3**) from list caused a significant improved. This can be related to difference in the pattern of the electrochemical behavior and electron transfer mechanism of **3** with other catechols. This compound during the oxidation can be converted to their tautomeric *p*-quinone methide (**3b**) form (Scheme 3) [31].

Table 2. The relations between $E_{1/2}$ (or E_{pa}) and E_{HOMO} in v = 600 mV/s.

$E_{1/2}$ *vs.* E_{HOMO}	E_{pa} *vs.* E_{HOMO}
5) $E^{a}_{1/2} = -0.6759 - 4.8374E_{HOMO}$	**7**) $E^{a}_{pa} = -0.4888 - 4.2959E_{HOMO}$
$R^2 = 0.5589$	$R^2 = 0.5374$
6) $E^{b}_{1/2} = -0.927 - 5.9664E_{HOMO}$	**8**) $E^{b}_{pa} = -0.725 - 5.3584E_{HOMO}$
$R^2 = 0.8394$	$R^2 = 0.8390$

[a]All **1-16** compounds.
[b]Without 4-methylcatechol (**3**).

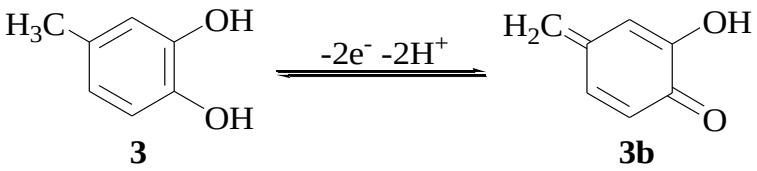

3 **3b**

Scheme 3.

Table 3 presents the calculated half-wave potentials by Eq. 4, in Table 1, in comparison with experimental values. A significant improvement can be seen for all of the catechols and the root-mean-square of errors (calculated without 3,4-dihydroxybenzonitril (**12**)) is less than 0.027 V. Therefore, if an E_{LUMO} for a new catechol derivative is calculated, the Eq. 4 can help to estimate the $E_{1/2}$ of this compound.

Table 3. Half-wave potential of the studied catechols calculated at the level of #B3LYP/6-311+G**, compared with the experimental values.

Catechol[a]	E_{LUMO} (eV)	$E_{1/2}$[b] (V)	$E_{1/2}$ (Experimenal) (V)
1	-0.01633	0.3766	0.3550
2	-0.01872	0.3821	0.3735
3	-0.01660	0.3772	0.3605
4	-0.00843	0.3585	0.3625
5	-0.01434	0.3720	0.3675
6	-0.04246	0.4365	0.3820
7	-0.02506	0.3966	0.4045
8	-0.05257	0.4596	0.5175
9	-0.03739	0.4249	0.4180
10	-0.02174	0.3890	0.4240
11	-0.07461	0.5101	0.5170
12	-0.05838	0.4730	0.5675
13	-0.07783	0.5175	0.5530
14	-0.11884	0.6115	0.5890
15	-0.08648	0.5373	0.5130
16	-0.07043	0.5006	0.5135

[a]See Fig. 1 for the list of studied catechols.
[b]Half-wave potentials calculated by Eq. 4.

4. CONCLUSION

The chemical structure of 16 catechol derivatives has been optimized by using of Gaussian 98 program and Quantum Mechanical Calculation Ab Initio. Optimization was performed at the #B3LYP/6-311+G** level. The half-wave potential, $E_{1/2}$, was correlated with the calculated energies of lowest unoccupied molecular orbital (E_{LUMO}) and highest occupied molecular orbital (E_{HOMO}) of the compounds studies. The simple linear relationship between $E_{1/2}$ and E_{HOMO} (or E_{LUMO}) for a series of compounds, demonstrates that they have a similar mechanism of the electron transfer reaction during electron transfer reaction. Because of the deviation of $E_{1/2}$ from its reversible (actual) amount in lower scan rates, the best relationship obtained in higher scan rates. This relation can be used for calculation of $E_{1/2}$ of new catechol derivatives. In correlations of $E_{1/2}$ with $E_{LUMO,}$ catechols with electron-withdrawing groups such as 3,4-dihydroxybenzonitril (**12**) because of the higher reactivity of related *o*-benzoquinone and participation in following chemical reactions such as hydroxylation, dimmerization and oxidative ring cleavage reactions are problematical. In addition, in correlations of $E_{1/2}$ (or E_{pa}) with $E_{HOMO,}$ 4-methylcatechol (**3**) has a large error, and its data are deleted. This can be related to different electro-oxidation behavior of 4-methylcatechol and formation of its tautomeric *p*-quinone methide.

ACKNOWLEDGEMENTS
The authors acknowledge to Bu-Ali Sina University Research Council and Center of Excellence in Development of chemical Methods (CEDCM) for support this work.

References

1. N. Schweigert, A. J. B. Zehnder and R. I. L. Eggen, *Environ. Microbiol.*, 3 (2001) 81.
2. R. H. Blum and S. K. Carter, *Ann. Int. Med.*, 80 (1974) 249.
3. AMICBASE-EssOil, Database on Natural Antimicrobials, Review Science, Germany, 1999-2002.
4. D. Nematollahi, M. Rafiee and L. Fotouhi, *J. Iran. Chem. Soc.*, 6 (2009) 448.
5. J. B. Raoof, R. Ojani, D. Nematollahi and A. Kiani, *Int. J. Electrochem. Sci.*, 4 (2009) 810.
6. D. Nematollahi, E. Tammari and H. Karbasi, *Int. J. Electrochem. Sci.*, 2 (2007) 986.
7. D. Nematollahi, M. Rafiee and A. Samadi-Maybodi, *Electrochim. Acta* 49 (2004) 2495.
8. M. D. Ryan, A. Yueh and C. Wen-Yu, *J. Electrochem. Soc.*, 127 (1980) 1489.
9. L. Papouchado, G. Petrie and R. N. Adams, *J. Electroanal. Chem.*, 38 (1972) 389.
10. L. Papouchado, G. Petrie, J. H. Sharp and R. N. Adams, *J. Am. Chem. Soc.*, 90 (1968) 5620.
11. T. E. Young, J. R. Griswold and M. H. Hulbert, *J. Org. Chem.*, 39 (1974) 1980.
12. T. R. Demmin, M. D. Swerdloff and M. M. Rogic, *J. Am. Chem. Soc.*, 103 (1981) 5795.
13. G. Lin, G. Reid and T. D. H. Bugg, C*hem. Commun.*, (2000) 1119.
14. D. Nematollahi and L. Mohammadi-Behzad, *Int. J. Electrochem. Sci.*, 4 (2009) 1583.
15. K. Izutsu, *Electrochemistry in nonaqueous solutions*, 1st Ed, Wiley, New York, 2001, p. 257 and 246.
16. J. E. Heffner, C. T**.** Wigal and O. A**.** Moe, *Electroanalysis* 9 (1997) 629.
17. K. Sasaki, T. Kashimura, M. Ohura, Y. Ohsaki and N. Qhta, *J. Electrochem. Soc.*, 137 (1990) 2437.
18. F. D. Saeva and G. R. Olin, *J. Am. Chem. Soc.*, 102 (1980) 299.
19. R. E. Sioda and B. Frankowska, *J. Electroanal. Chem.*, 612 (2008) 147.
20. S. Okazaki, M. Oyama and S. Nomura, *Electroanalysis* 9 (1997) 1242.
21. R. E. Sioda and B. Frankowska, *J. Electroanal. Chem.*, 568 (2004) 365.

22. J. E. Heffner, J. C. Raber, O. A. Moe and C. T. Wigal, *J.Chem. Ed.*, 75 (1988) 365.
23. S. Riahi, M. R. Ganjali, A. Bayandori Moghaddam, P. Norouzi and M. Niasari, *Theochem.*, 774 (2006) 107.
24. S. Riahi, M. R. Ganjali, H. Khajehsharifi, P. Norouzi and S. Taghipoor, *Int. J. Electrochem. Sci.*, 4 (2009) 122.
25. J. Bard and L. R. Faulkner, *Electrochemical Methods*, 2nd Ed, Wiley, New York, 2001, p. 497.
26. D. Nematollahi and H. Shayani-Jam, *J. Org. Chem.*, 73 (2008) 3428.
27. D. Nematollahi, M. Alimoradi and M. Rafiee, *J. Phys. Org. Chem.*, 20 (2007) 49.
28. D. Nematollahi, M. Alimoradi and S. Waqif Husain, *Electroanalysis* 16 (2004) 1359.
29. D. Nematollahi, A. Ariapad and M. Rafiee, *J. Electroanal. Chem.*, 602 (2007) 37.
30. L. Fotouhi, E. Tammari, S. Asadi, M. M. Heravi and D. Nematollahi, *Int. J. Chem. Kinet.*, 41 (2009) 426.
31. M. Sugumaran and H. Lipke, *FEBS Lett.*, 155 (1983) 65.